EARTHQUAKE ENGINEERING AND STRUCTURAL DYNAMICS, VOL. 25, 1–13 (1996)

ENVELOPE OF GREEN'S FUNCTION FOR STRUCTURAL RESPONSE WITH SLIGHTLY DETUNED VIBRATION ABSORBERS

HSIANG-CHUAN TSAI*

Department of Construction Engineering, National Taiwan Institute of Technology, P.O. Box 90-130, Taipei, Taiwan, R.O.C.

SUMMARY

Explicit forms of the modal parameters and the envelope of the Green's function for transient response of main structures equipped with vibration absorbers are derived using a perturbation technique and assuming that the natural frequency of the absorber is slightly detuned from that of the main structure. Applying these perturbation solutions, the influence of the absorber parameters on the dynamic response of main structures is investigated and the ratio of the envelope for the main mass with absorber to that without absorber is constructed to provide insight to evaluate the effectiveness of the absorber to diminish the vibrations of main structures.

KEY WORDS: vibration absorber; damping; Green's function; perturbation

INTRODUCTION

The vibration absorber, also called a tuned-mass damper, is a classical engineering device consisting of a mass, a spring and a viscous damper attached to a vibrating main structure in order to attenuate undesirable vibrations. The natural frequency of the absorber is tuned to a frequency near the natural frequency of the main structure. Because the light mass of the absorber vibrates much more violently than the heavy mass of the main structure, the vibration energy can be dissipated through the damping in the absorber.

There is extensive work on the steady-state response of structures equipped with absorbers and subjected to harmonic excitation[1–5]. The transient response of structures with absorbers subjected to short-impulse support excitation, the Green's function of general support excitation, was derived through a perturbation approach;[6] the magnitude of the detuning parameter, which represents the difference between the natural frequency of the main structure and that of the absorber, was assumed to be of the same order as the magnitude of the ratio of the absorber mass to the main mass. The major term of the Green's function was found to be independent of the detuning parameter, which means that the results are applicable to the nearly tuned absorber.

In the present work we put emphasis on the response of structures with slightly detuned absorbers. The magnitude of the detuning parameter is assumed to be of the order of the square root of the mass ratio. Hence, the absorber has more detuning in the current paper than in the previous one.[6] If the mass ratio is 0·01, the Green's function derived in Reference 6 is available for the detuning parameter near to or below 0·01 while the solution presented in the current paper is suitable for the detuning parameter up to 0·1.

Following the analytic approach and perturbation technique described earlier,[6] the explicit forms of the modal parameters and the envelope of the Green's function of structural response for the slightly detuned absorber are derived. Applying these perturbed solutions, the influence of the tuning frequency and the absorber damping on the effectiveness of the absorber are investigated.

---

* Associate Professor

CCC 0098–8847/96/010001–13

Received 3 January 1995
Revised 9 May 1995

PERTURBED SOLUTIONS

The model support-excited structure with absorber is shown in Figure 1 in which the main structure is simplified as a lump mass m_p with stiffness k_p and damping c_p. The absorber has mass m_s, stiffness k_s and damping c_s. Let u_p represent the displacement of the main mass relative to the ground and u_s be that of the absorber. The equation of motion for the model excited by the ground acceleration, $\ddot{u}_g$, is established as

$$\begin{bmatrix} m_p & 0 \\ 0 & m_s \end{bmatrix} \begin{Bmatrix} \ddot{u}_p \\ \ddot{u}_s \end{Bmatrix} + \begin{bmatrix} c_p + c_s & -c_s \\ -c_s & c_s \end{bmatrix} \begin{Bmatrix} \dot{u}_p \\ \dot{u}_s \end{Bmatrix} + \begin{bmatrix} k_p + k_s & -k_s \\ -k_s & k_s \end{bmatrix} \begin{Bmatrix} u_p \\ u_s \end{Bmatrix} = -\begin{Bmatrix} m_p \\ m_s \end{Bmatrix} \ddot{u}_g \tag{1}$$

which can be simply expressed in terms of matrix notation

$$\mathbf{M}\ddot{\mathbf{u}} + \mathbf{C}\dot{\mathbf{u}} + \mathbf{K}\mathbf{u} = -\mathbf{M}\mathbf{r}\ddot{u}_g \tag{2}$$

The natural frequencies of the main mass and of the absorber are defined by $\omega_p = \sqrt{k_p/m_p}$ and $\omega_s = \sqrt{k_s/m_s}$, respectively. Their associated damping ratios are given by $\xi_p = c_p/2\omega_p m_p$ and $\xi_s = c_s/2\omega_s m_s$, respectively.

The properties of the absorber are described in terms of three non-dimensional parameters. The mass parameter

$$\gamma = m_s/m_p \tag{3}$$

is the ratio of the absorber mass to the main mass. The damping parameter

$$\xi_d = \xi_s - \xi_p \tag{4}$$

is the damping difference between the absorber and the main structure. The detuning parameter

$$\beta = 2(\omega_p - \omega_s)/(\omega_p + \omega_s) \tag{5}$$

represents the frequency difference between the absorber and the main structure. In order to utilize perturbation principles, the relative order of magnitude of each parameter must be established. In general, the absorber mass is much smaller than the main mass, so that the mass parameter, γ, is a small quantity. Neglecting its higher-order terms does not seriously affect the accuracy for engineering applications. It is assumed that ξ_p and ξ_d are of order $\sqrt{\gamma}$. The natural frequency of the absorber is near the natural frequency

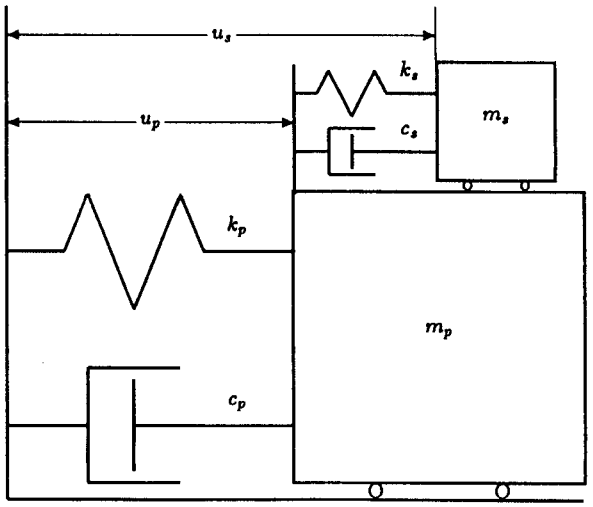

Figure 1. The main mass with a vibration absorber

of the main structure so that the detuning parameter, which has the following relation with the frequency ratio,

$$f = \frac{\omega_s}{\omega_p} \approx 1 - \beta \tag{6}$$

is a small quantity. In our previous work,[6] β was assumed to be of order γ. To investigate the Green's function in the slightly detuned condition, β is assumed to be of order $\sqrt{\gamma}$ in the present work.

The complex mode method[6] is applied to solve equation (2). The eigenvalues p_i and eigenvectors $\mathbf{\Phi}_i$ of equation (2), which satisfy the following characteristic equation:

$$(p_i^2\mathbf{M} + p_i\mathbf{C} + \mathbf{K})\mathbf{\Phi}_i = \mathbf{0} \tag{7}$$

are complex in value and occur in conjugate pairs. Using the perturbation technique,[6] the major terms of eigenvalues are derived as

$$p_1 \approx \omega_p(-\xi_p - \tfrac{1}{2}\xi_d + \tfrac{1}{2}\delta) + i\omega_p(1 - \tfrac{1}{2}\beta + \tfrac{1}{2}\varepsilon) \tag{8}$$

$$p_3 \approx \omega_p(-\xi_p - \tfrac{1}{2}\xi_d - \tfrac{1}{2}\delta) + i\omega_p(1 - \tfrac{1}{2}\beta - \tfrac{1}{2}\varepsilon) \tag{9}$$

in which δ and ε are of order $\sqrt{\gamma}$ and are defined by

$$\delta = \sqrt{\frac{1}{2}[\sqrt{(\gamma + \beta^2 - \xi_d^2)^2 + 4\beta^2\xi_d^2} - (\gamma + \beta^2 - \xi_d^2)]} \tag{10}$$

$$\varepsilon = \frac{\beta\xi_d}{\delta} = \operatorname{sgn}(\beta\xi_d)\sqrt{\frac{1}{2}[\sqrt{(\gamma + \beta^2 - \xi_d^2)^2 + 4\beta^2\xi_d^2} + (\gamma + \beta^2 - \xi_d^2)]} \tag{11}$$

in which $\operatorname{sgn}(\beta\xi_d)$ is the algebraic sign of $\beta\xi_d$. The other eigenvalues, p_2 and p_4, are the conjugates of p_1 and p_3, respectively. The eigenvectors are

$$\mathbf{\Phi}_1 \approx \begin{Bmatrix} 1 \\ \frac{1}{\gamma}[(\beta - \varepsilon) + i(-\xi_d + \delta)] \end{Bmatrix} \tag{12}$$

$$\mathbf{\Phi}_3 \approx \begin{Bmatrix} 1 \\ \frac{1}{\gamma}[(\beta + \varepsilon) + i(-\xi_d - \delta)] \end{Bmatrix} \tag{13}$$

in which the component corresponding to the displacement of the main mass is normalized to be unity.

The participation factor of each eigenvector N_i is defined by[6]

$$N_i = \frac{\mathbf{\Phi}_i^T\mathbf{M}\mathbf{r}}{2p_i\mathbf{\Phi}_i^T\mathbf{M}\mathbf{\Phi}_i + \mathbf{\Phi}_i^T\mathbf{C}\mathbf{\Phi}_i} \tag{14}$$

By substituting the major terms of eigenvalues and eigenvectors into the above equation, we find the major terms of N_i to be

$$N_1 \approx \frac{1}{4\omega_p}[-a - i(1 + b)] \tag{15}$$

$$N_3 \approx \frac{1}{4\omega_p}[a - i(1 - b)] \tag{16}$$

in which

$$a = \frac{(\gamma + \beta^2 - \xi_d^2)(\xi_d\varepsilon + \beta\delta) - 2\beta\xi_d(\beta\varepsilon - \xi_d\delta)}{(\gamma + \beta^2 - \xi_d^2)^2 + (2\beta\xi_d)^2} \tag{17}$$

and

$$b = \frac{(\gamma + \beta^2 - \xi_d^2)(\beta\varepsilon - \xi_d\delta) + 2\beta\xi_d(\xi_d\varepsilon + \beta\delta)}{(\gamma + \beta^2 - \xi_d^2)^2 + (2\beta\xi_d)^2} \tag{18}$$

The magnitudes of a and b are of order γ^0.

The displacement of the main mass is obtained by the combination of the corresponding responses of all eigenvectors. As p_i and N_i are complex and occur in conjugate pairs, the combination cancels the imaginary part and reduces the displacement of the main mass to be of the form

$$u_p = \sum_{i=1}^{2} \int_0^t \exp(\Re(p_{2i-1})(t-\tau))[-2\Re(N_{2i-1})\cos(\Im(p_{2i-1})(t-\tau)) + 2\Im(N_{2i-1})\sin(\Im(p_{2i-1})(t-\tau))]\ddot{u}_g(\tau)\mathrm{d}\tau \tag{19}$$

in which $\Re(\,)$ and $\Im(\,)$ are the real and imaginary parts of a complex number, respectively.

MODAL PARAMETERS

The eigenvalues have the following relationship to the undamped modal frequencies ω_i and damping ratios[7] ξ_i

$$p_{2i-1} = -\xi_i\omega_i + \mathrm{i}\omega_i\sqrt{(1-\xi_i^2)}; \qquad p_{2i} = -\xi_i\omega_i - \mathrm{i}\omega_i\sqrt{(1-\xi_i^2)} \tag{20}$$

According to the major terms of the complex eigenvalues in equations (8) and (9), the major terms of undamped modal frequencies are obtained as

$$\omega_1 \approx \omega_p(1 - \tfrac{1}{2}\beta + \tfrac{1}{2}\varepsilon); \qquad \omega_2 \approx \omega_p(1 - \tfrac{1}{2}\beta - \tfrac{1}{2}\varepsilon) \tag{21}$$

The major terms of the corresponding damping ratios are

$$\xi_1 \approx \xi_p + \tfrac{1}{2}\xi_d - \tfrac{1}{2}\delta; \qquad \xi_2 \approx \xi_p + \tfrac{1}{2}\xi_d + \tfrac{1}{2}\delta \tag{22}$$

Here, ω_1 and ξ_1 are derived from the first conjugate pair of eigenvalues and are referred to henceforth as the natural frequency and damping ratio of the first mode. ω_2 and ξ_2, derived from the second conjugate pair, are referred to as the natural frequency and damping ratio of the second mode.

The variations of $(\omega_i/\omega_p) - (1 - 0{\cdot}5\beta)$ and $\xi_i - (\xi_p + 0{\cdot}5\xi_d)$ with ξ_d for various β are plotted in Figures 2(a) and 2(b), respectively, which demonstrate the differences of modal frequencies and damping ratios between the two modes. According to ε defined in equation (11), two modal frequencies in $\gamma + \beta^2 - \xi_d^2 > 0$ have a larger difference than those in $\gamma + \beta^2 - \xi_d^2 < 0$. The difference of damping ratios between the two

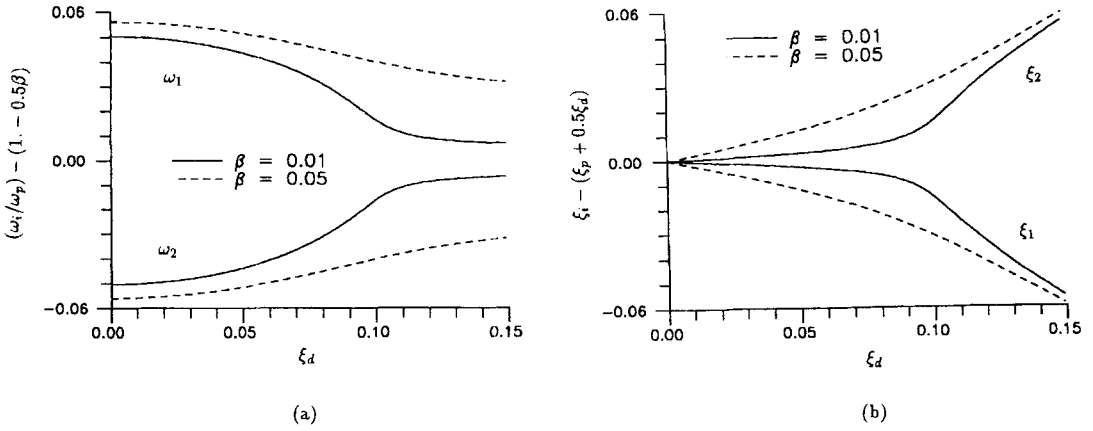

Figure 2. Variations of (a) modal frequencies and (b) damping ratios with damping parameter ($\gamma = 0{\cdot}01$)

modes, which is related to δ defined in equation (10), has a contrary variation. However, these variations diminish for larger β as shown in Figure 2(a). Similar situation has been found in Reference 6 where β is assumed to be of higher order so that the modal parameters have abrupt changes when ξ_d crosses the boundary of $\gamma - \xi_d^2 = 0$. It should be noted that, since ε and δ are not functions of ξ_p, the curves shown in Figure 2 become independent of ξ_p, which is different from the results shown in the earlier work,[6] where the modal parameters are solved up to the terms of order γ which contain ξ_p.

As the value of δ is invariably positive, the modal parameters illustrated in equations (21) and (22) ensure that the second mode has invariably a larger damping ratio than the first mode. If $\gamma - \xi_d^2 < 0$, these expressions have a smoothly varying modal frequency and damping ratio when β changes algebraic sign. If $\gamma - \xi_d^2 > 0$, however, as ε is not zero at $\beta = 0$, the modal frequency has an abrupt alteration when β changes sign. To eliminate the abrupt variation of frequencies, the expression of the modal frequencies are rearranged to

$$\omega_1 \approx \omega_p(1 - \tfrac{1}{2}\beta + \tfrac{1}{2}|\varepsilon|); \qquad \omega_2 \approx \omega_p(1 - \tfrac{1}{2}\beta - \tfrac{1}{2}|\varepsilon|) \tag{23}$$

The corresponding damping ratios become

$$\xi_1 \approx \xi_p + \tfrac{1}{2}\xi_d - \tfrac{1}{2}\mathrm{sgn}(\beta\xi_d)\delta; \qquad \xi_2 \approx \xi_p + \tfrac{1}{2}\xi_d + \tfrac{1}{2}\mathrm{sgn}(\beta\xi_d)\delta \tag{24}$$

The modal frequencies and damping ratios varying with β are plotted in Figure 3 according to equations (21) and (22) and in Figure 4, according to equations (23) and (24). These figures have the same parameters, $\omega_p = 0{\cdot}5$ Hz, $\xi_p = 0{\cdot}05$ and $\gamma = 0{\cdot}01$. Figure 3 has $\xi_d = 0{\cdot}12$ to satisfy the condition $\gamma - \xi_d^2 < 0$. Figure 4 has $\xi_d = 0{\cdot}05$ to satisfy the condition $\gamma - \xi_d^2 > 0$. Figures 3 and 4 reveal that, as the magnitude of β approaches zero, two modal frequencies become close together and converge to the same value if $\gamma - \xi_d^2 < 0$ and the damping ratios of two modes have a similar variation with β if $\gamma - \xi_d^2 > 0$.

Figures 3 and 4 also compare the perturbed solutions with the exact solutions computed from an eigensolver, which indicate that the differences between the two results are small. In the earlier work[6] in which β was assumed to be of order γ, the damping ratios are solved up to the order of γ for $\gamma - \xi_d^2 > 0$. However, only the term of order $\sqrt{\gamma}$ can be solved for the damping ratio, if β is of order $\sqrt{\gamma}$. To increase the accuracy, the term of order γ solved from the earlier work can be added to equation (24), which becomes

$$\xi_1 \approx \xi_p + \tfrac{1}{2}\xi_d - \tfrac{1}{2}\mathrm{sgn}(\beta\xi_d)\delta + \frac{\gamma(\xi_p + \xi_d)}{2\sqrt{\gamma - \xi_d^2}}; \qquad \xi_2 \approx \xi_p + \tfrac{1}{2}\xi_d + \tfrac{1}{2}\mathrm{sgn}(\beta\xi_d)\delta - \frac{\gamma(\xi_p + \xi_d)}{2\sqrt{\gamma - \xi_d^2}} \tag{25}$$

Figure 5 compares the results of the above two equations with the exact solutions and indicates that the perturbation error is further decreased.

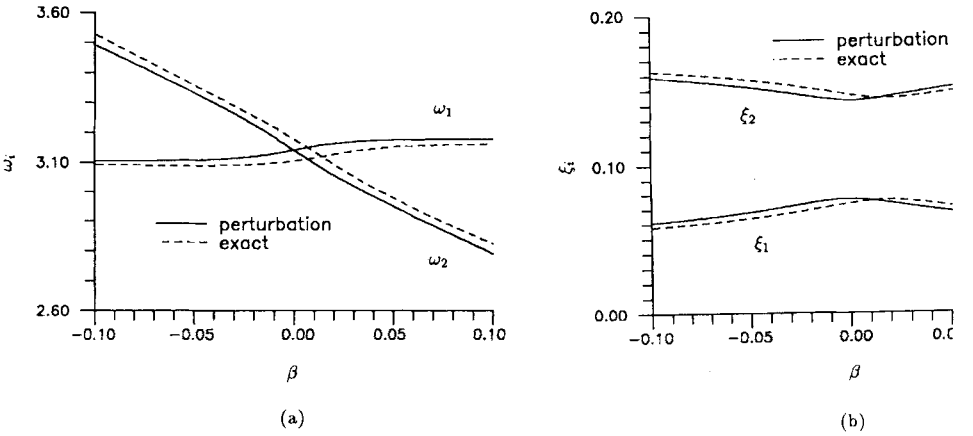

Figure 3. Variations of (a) modal frequencies and (b) damping ratios with detuning parameter for $\gamma - \xi_d^2 < 0$ ($\omega_p = 0{\cdot}5$ Hz, $\xi_p = 0{\cdot}05$, $\gamma = 0{\cdot}01$ and $\xi_d = 0{\cdot}12$)

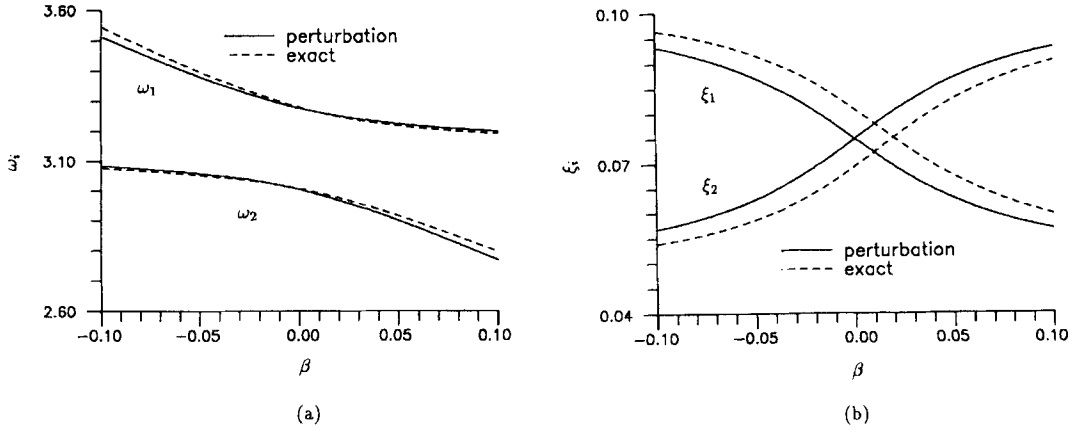

Figure 4. Variations of (a) modal frequencies and (b) damping ratios with detuning parameter for $\gamma - \xi_d^2 > 0$ ($\omega_p = 0{\cdot}5$ Hz, $\xi_p = 0{\cdot}05$, $\gamma = 0{\cdot}01$ and $\xi_d = 0.05$)

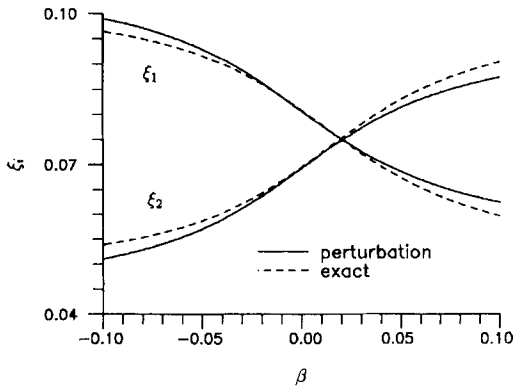

Figure 5. Comparison of damping ratios in equation (24) with exact solutions ($\omega_p = 0{\cdot}5$ Hz, $\xi_p = 0{\cdot}05$, $\gamma = 0{\cdot}01$ and $\xi_d = 0{\cdot}05$)

The modal frequencies and damping ratios for the system with two degrees of freedom are solved in published papers that describe the equipment-structure system,[8,9] for which the orders of β and ξ_d are set to be the same as those assumed in the present work. Hence their solutions are similar or equivalent to those presented here. However, the algebraic sign of $\beta\xi_d$ in equation (11) was ignored in Reference 8, which might instigate the wrong correlation between modal frequencies and damping ratios of the two modes. Equations (23) and (24) are mathematically identical to the solutions given in Reference 9, which use complex-valued expressions, from which it is difficult to calculate numerical values. Figures 2–5 show the variation of the model parameters with the detuning parameter. Some similar results have been given in the literature, but plotted modal parameters of Fujino and Abé (Figures 2–4 of Reference 10) are for zero structural damping and Igusa and Der Kiureghian[9] plot the variation of modal parameters only for a positive detuning parameter for the case when $\gamma > \xi_d^2$.

ENVELOPE OF GREEN'S FUNCTION

The displacement of the main mass in equation (19) is simply expressed as

$$u_p = \int_0^t G(t-\tau)\ddot{u}_g(\tau)\,d\tau \tag{26}$$

in which $G(t)$ is the Green's function of u_p and is derived approximately from the perturbed solution of p_i and N_i,

$$G(t) \approx -\frac{1}{\omega_p}[A_1 \exp(-(\xi_p + \tfrac{1}{2}\xi_d - \tfrac{1}{2}\delta)\omega_p t)\sin((1 - \tfrac{1}{2}\beta + \tfrac{1}{2}\varepsilon)\omega_p t - \theta_1) + A_2 \exp(-(\xi_p + \tfrac{1}{2}\xi_d + \tfrac{1}{2}\delta)\omega_p t)\sin((1 - \tfrac{1}{2}\beta - \tfrac{1}{2}\varepsilon)\omega_p t + \theta_2)] \tag{27}$$

in which

$$A_1 = \tfrac{1}{2}\sqrt{(1+b)^2 + a^2}; \qquad A_2 = \tfrac{1}{2}\sqrt{(1-b)^2 + a^2} \tag{28}$$

$$\theta_1 = \tan^{-1}\left(\frac{a}{1+b}\right); \qquad \theta_2 = \tan^{-1}\left(\frac{a}{1-b}\right) \tag{29}$$

The terms of A_1 and A_2 in equation (27) represent the contribution of the first and second modes, respectively. These two terms are further combined to

$$G(t) \approx -\frac{1}{\omega_p}\rho A_1 \exp(-(\xi_p + \tfrac{1}{2}\xi_d - \tfrac{1}{2}\delta)\omega_p t)\sin((1 - \tfrac{1}{2}\beta)\omega_p t + \tfrac{1}{2}(\theta_2 - \theta_1) + \psi) \tag{30}$$

in which

$$\rho = \sqrt{\left(1 - \frac{A_2}{A_1}\exp(-\delta\omega_p t)\right)^2 + 4\frac{A_2}{A_1}\exp(-\delta\omega_p t)\cos^2\left(\frac{\varepsilon\omega_p t - \theta_1 - \theta_2}{2}\right)} \tag{31}$$

$$\psi = \tan^{-1}\left(\frac{1 - \dfrac{A_2}{A_1}\exp(-\delta\omega_p t)}{1 + \dfrac{A_2}{A_1}\exp(-\delta\omega_p t)}\tan\left(\frac{\varepsilon\omega_p t - \theta_1 - \theta_2}{2}\right)\right) \tag{32}$$

Figure 6 shows the Green's function of a system having $\omega_p = 0{\cdot}5$ Hz, $\xi_p = 0{\cdot}02$, $\gamma = 0{\cdot}01$, $\xi_d = 0{\cdot}02$ and $\beta = 0{\cdot}05$. Also plotted in this figure is the envelope of the Green's function, defined as

$$E(t) \approx \frac{1}{\omega_p}\rho A_1 \exp(-(\xi_p + \tfrac{1}{2}\xi_d - \tfrac{1}{2}\delta)\omega_p t) \tag{33}$$

The envelope of the Green's function for the response of the main mass without the absorber is derived as[6]

$$E^*(t) \approx \frac{1}{\omega_p}\exp(-\xi_p\omega_p t) \tag{34}$$

The effectiveness of the absorber to decrease vibration of the main mass is evaluated from the ratio of the envelopes defined as

$$R(t) = \frac{E(t)}{E^*(t)} \approx \rho A_1 \exp\left(-\frac{\xi_d - \delta}{2}\omega_p t\right) \tag{35}$$

It should be noted that, because the higher-order terms have been neglected, the envelope ratio becomes independent of ξ_p. In other words, the influence of structural damping on the envelope ratio is minor.

The influence of absorber parameters on the envelope ratio was explored from the three factors shown in equation (35). A larger value of $\xi_d - \delta$ in the exponential term causes a more rapid decay of $R(t)$. The variations of $\xi_d - \delta$ with β for four ξ_d are plotted in Figure 7(a) that reveals $\xi_d - \delta$ to decrease with increasing β. The variations of $\xi_d - \delta$ with ξ_d for four β are plotted in Figure 7(b) that shows $\xi_d - \delta$ to attain a maximum when ξ_d is close to $\sqrt{\gamma}$ and a smaller β to have a sharper maximum.

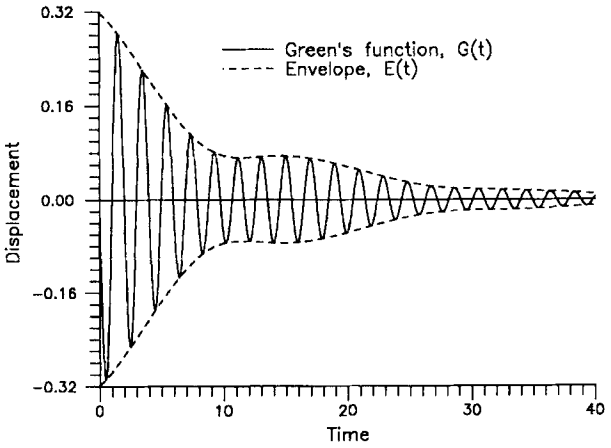

Figure 6. Green's function and its envelope ($\omega_p = 0{\cdot}5$ Hz, $\xi_p = 0{\cdot}02$, $\gamma = 0{\cdot}01$, $\xi_d = 0{\cdot}02$ and $\beta = 0{\cdot}05$)

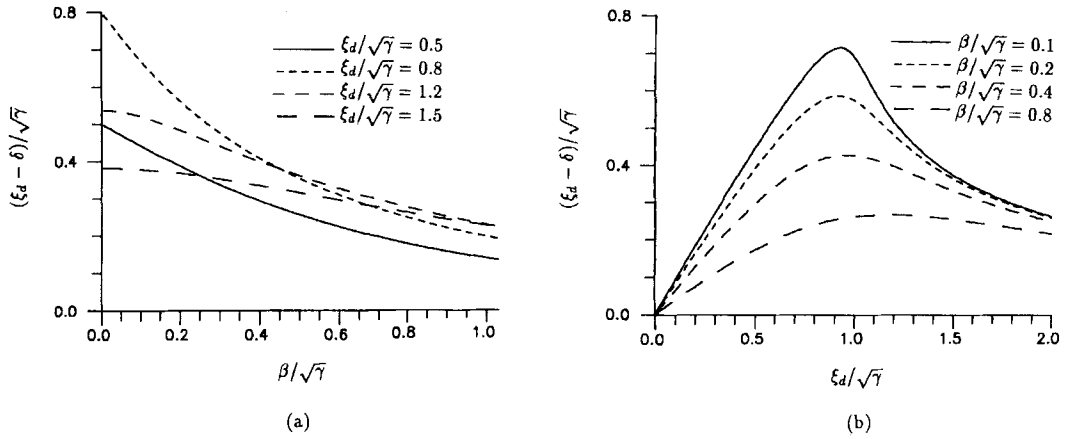

Figure 7. Variations of $\xi_d - \delta$ with (a) β and (b) ξ_d

The second factor A_1 is the amplitude of the first mode that has a smaller damping ratio than the second mode. The variations of A_1 with β are plotted in Figure 8(a) that reveals A_1 to approach unity as β grows. The variations of A_1 with ξ_d are plotted in Figure 8(b) that indicates that, when $\xi_d < 0{\cdot}8\sqrt{\gamma}$, smaller β has smaller A_1. However, when $\xi_d > 0{\cdot}8\sqrt{\gamma}$, smaller β has a higher maximum of A_1.

The third factor ρ, that denotes interference of the second mode with the first mode, is a function of $\omega_p t$ shown in equation (31). In this equation, the contribution of the amplitude ratio A_2/A_1 decays with increasing time because of the exponential term $\exp(-\delta\omega_p t)$. The variations of A_2/A_1 and δ with β are plotted in Figure 9(a) and 9(b), respectively, which reveal that, with increasing β, A_2/A_1 decreases and δ increases. Therefore, increasing β diminishes the contribution of the second mode.

According to equation (31), ρ fluctuates between $1 + (A_2/A_1)\exp(-\delta\omega_p t)$ and $1 - (A_2/A_1)\exp(-\delta\omega_p t)$. The frequency of the fluctuation depends on the coefficient ε in the cosine term of equation (31). Figure 10(a) reveals that larger β or smaller ξ_d makes ρ fluctuate at an increased frequency. The phase angle $\theta_1 + \theta_2$, that affects the ρ value in the early stage of vibration, is plotted in Figure 10(b) that shows the phase angle to decrease with increasing β or decreasing ξ_d.

If β is decreased to be of order γ, the coefficients defined in the previous sections will neglect the terms of β and the Green's function will develop into the expression presented in Reference 6. When $\xi_d > \sqrt{\gamma}$, the two

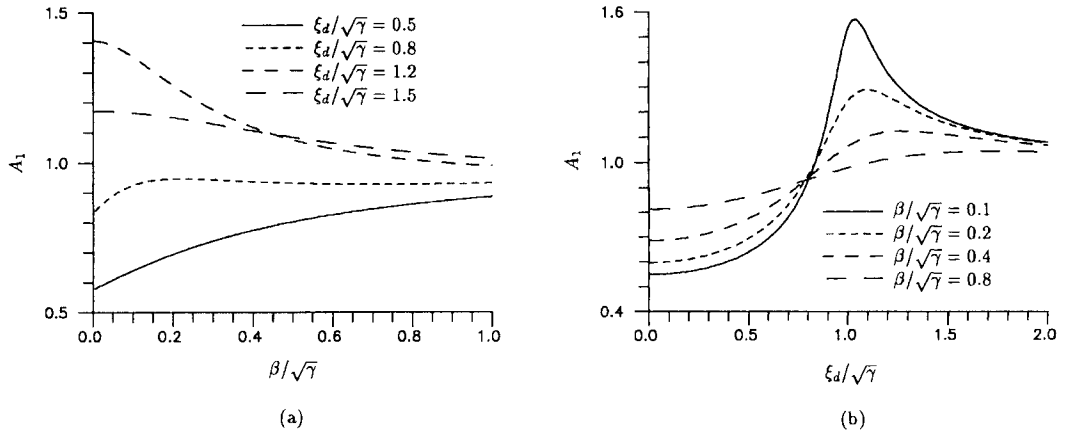

Figure 8. Variations of A_1 with (a) β and (b) ξ_d

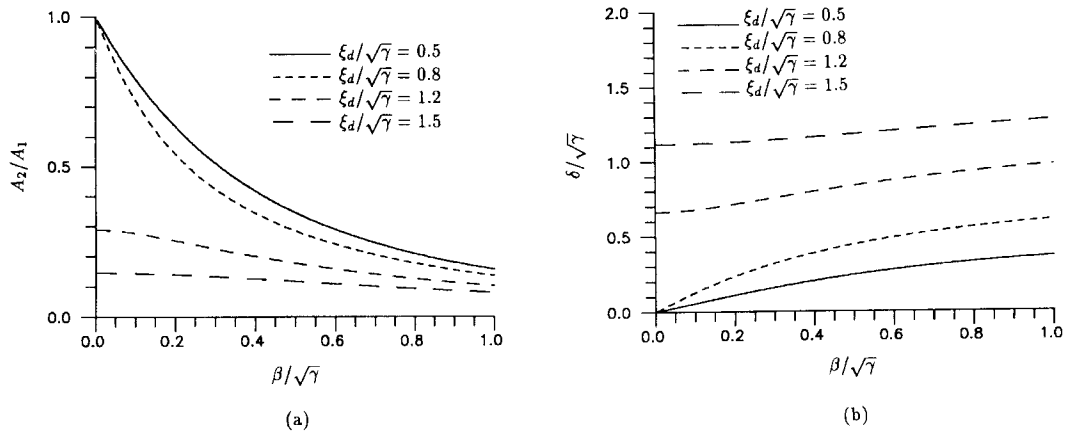

Figure 9. Variations of (a) A_2/A_1 and (b) δ with β

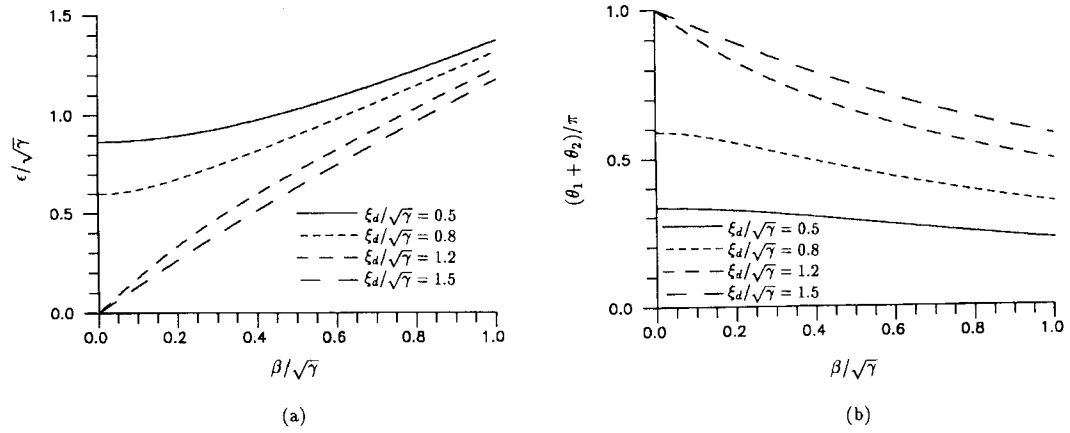

Figure 10. Variations of (a) ε and (b) $\theta_1 + \theta_2$ with β

modes have the same frequency as shown in Figure 3 and the contribution of the second mode, which has a greater damping ratio, becomes damped. When $\xi_d < \sqrt{\gamma}$, decreasing β leads the two modes to have the same damping ratio as shown in Figure 4 and the same amplitude, $A_1 \approx A_2$, so that the two modes play the same prominent role and make the value of ρ fluctuate by a frequency equal to the difference of the two modal frequencies. Since the frequency difference is a small quantity, the Green's function will show the beat phenomenon described in Reference 6.

To support the above deductions, we plot the variations of ρA_1 with t/T_p, in which $T_p = 2\pi/\omega_p$, in Figure 11(a) for four ξ_d with the same $\beta(= 0{\cdot}02)$ and $\gamma(= 0{\cdot}01)$. For any values of the parameters, $\rho A_1 = 1$ at $t = 0$ and, as $t = \infty$, $\rho A_1 = A_1$. Figure 11(a) shows that, when $\xi_d > \sqrt{\gamma}$, ρA_1 converges rapidly to A_1. As $\xi_d = 0{\cdot}05$ has a greater value of ε than $\xi_d = 0{\cdot}08$, the curve of $\xi_d = 0{\cdot}05$ fluctuates with a higher frequency. Note $\xi_d = 0{\cdot}05$ also has a smaller value of $\theta_1 + \theta_2$, which makes the curve of $\xi_d = 0{\cdot}05$ decay earlier than the curve of $\xi_d = 0{\cdot}08$. Figure 11(b) compares the ρA_1 curves of various β for the same $\xi_d = 0{\cdot}08$ and $\gamma = 0{\cdot}01$, which shows that a greater β converges more rapidly to A_1.

The solution derived by the perturbation technique provides an easy approach to construct the curves of the envelope ratio, $R(t)$. Figures 12(a) and 12(b) show the envelope ratios for $\beta = 0{\cdot}01$ and $\beta = 0{\cdot}04$,

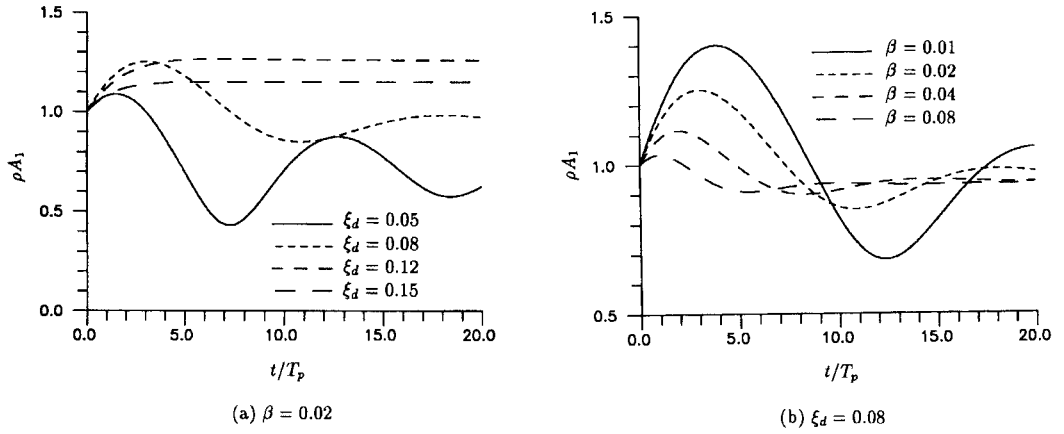

(a) $\beta = 0.02$ (b) $\xi_d = 0.08$

Figure 11. Variations of ρA_1 with t/T_p ($\gamma = 0{\cdot}01$)

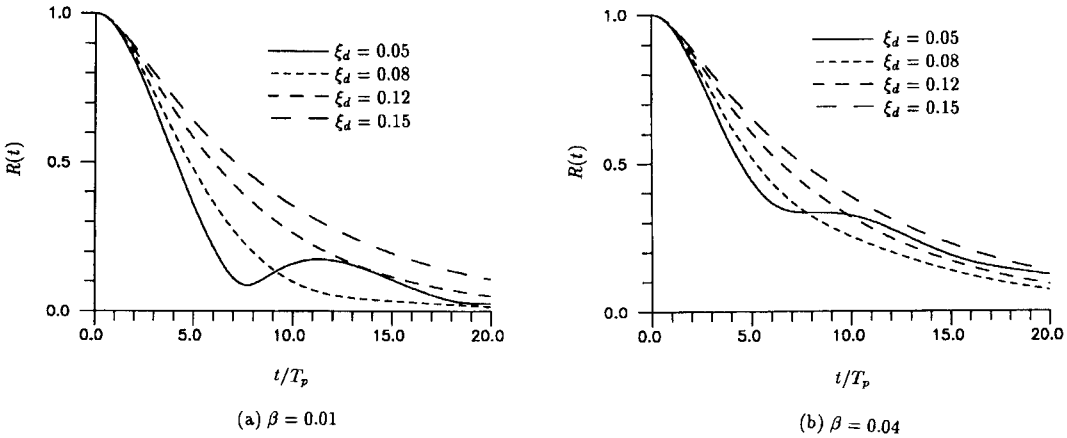

(a) $\beta = 0.01$ (b) $\beta = 0.04$

Figure 12. Comparison of envelope ratio between different ξ_d ($\gamma = 0{\cdot}01$)

respectively, with the same $\gamma = 0{\cdot}01$. These figures reveal that a greater ξ_d has a greater value of $R(t)$ except for $\xi_d = 0{\cdot}05$. Because of the high fluctuation frequency of ρ, the curve for $\xi_d = 0{\cdot}05$ rebounds after decaying rapidly during the first seven periods. Comparing Figure 12(a) with Figure 12(b), we discern that the influence of ξ_d on $R(t)$ is diminished as β is increased. The curves of envelope ratios of various β are compared in Figures 13(a) and 13(b) for $\xi_d = 0{\cdot}05$ and $\xi_d = 0{\cdot}08$, respectively, with the same $\gamma = 0{\cdot}01$, which indicates that the effectiveness of the vibration absorber is decreased for a large value of β.

Since the amplitude of the Green's function for the structures without the absorber decays exponentially with time, the amount of Green's function reduced by the absorber is not necessary to increase with increasing time, even though the envelope ratio decreases with increasing time. Figure 14 shows the Green's functions for two different ξ_p. Both have the same absorber parameters, γ, ξ_d and β, so that they have the same envelope ratio. However, the amount of the Green's function reduced by the absorber is more prominent in $\xi_p = 0{\cdot}02$ than in $\xi_p = 0{\cdot}05$. Because the structure with lower ξ_p has larger response, the absorber becomes more promising to reduce the response of the structure having lower damping.

Figure 13 implies that, when the absorber is tuned, i.e. $\beta = 0$, the envelope ratio has the lowest values for a particular ξ_d. The results in Reference 6 and Figure 12 indicate that $\xi_d = \sqrt{\gamma}$ has the lowest envelope ratio among $\xi_d \geqslant \sqrt{\gamma}$, but, for $\xi_d \leqslant \sqrt{\gamma}$, a smaller ξ_d has a smaller envelope ratio in the first few periods but has

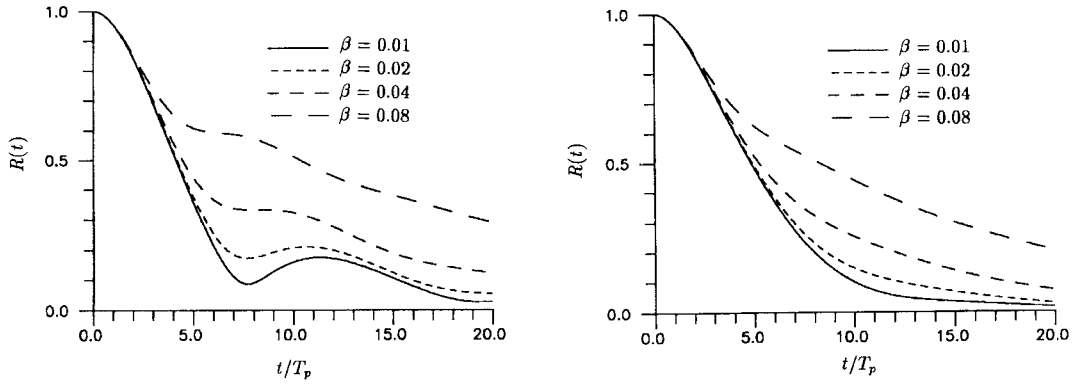

(a) $\xi_d = 0.05$ (b) $\xi_d = 0.08$

Figure 13. Comparison of envelope ratio between different β ($\gamma = 0{\cdot}01$)

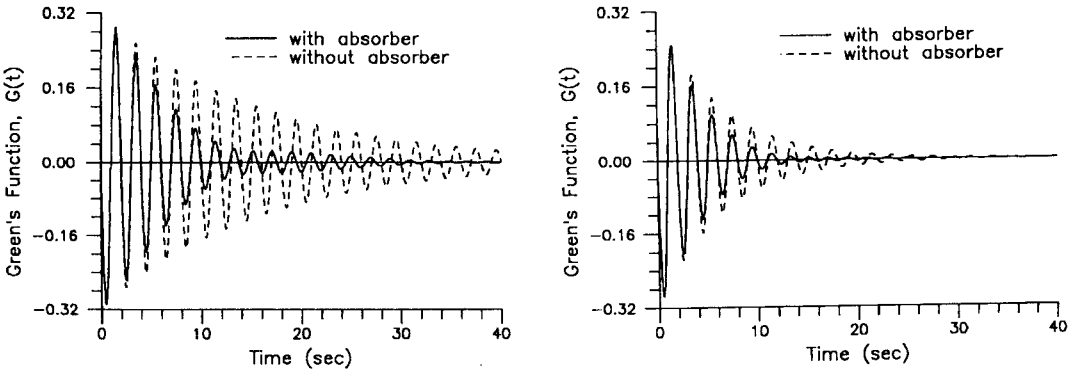

(a) $\xi_p = 0.02$ (b) $\xi_p = 0.05$

Figure 14. Green's functions for structures with absorber and without absorber ($\omega_p = 0{\cdot}5$ Hz, $\gamma = 0{\cdot}01$, $\xi_d = 0{\cdot}05$, $\beta = 0{\cdot}04$)

a higher rebound. Moreover, the envelope ratios as shown in Figures 12 and 13 always start from a value of unity at zero time for any value of the absorber parameters. Figure 14 exhibits that the addition of an absorber has very little effect on the first one or two response peaks. All these facts imply that the procedure to find the optimum parameters for the envelope ratio or the Green's function is not obvious. For the transient response, the optimum condition is to minimize the maximum response of u_p defined in equation (26). Equation (26) and numerical results[11] indicate that the maximum u_p also depends on the choice of acceleration input. Hence, deciding the optimum absorber parameters for the transient response is more difficult.

The structural response investigated in the present work is the displacement of the main mass. However, the absolute acceleration of the main mass is approximately proportional to the displacement response, $\ddot{u}_p^t = \ddot{u}_p + \ddot{u}_g \approx \omega_p^2 u_p$; hence the characteristics of the Green's function for absolute acceleration are similar to those presented here for displacement.

The excitation of the type considered here is the support motion. If the excitation source is the external force acting on the main mass, the component corresponding to the absorber in the loading vector of equation (1) becomes altered from order γ to zero. As the variation is minor, it does not affect the major terms of the participation factors shown in equations (15) and (16). Therefore, the Green's function for the force excitation is similar to those presented here for the support excitation and possesses the same characteristics.

CONCLUSION

The main structure with a vibration absorber has been simplified to a system with two degrees of freedom and solved according to the method of complex modes. As the mass ratio of the absorber and the main structure is small and as the natural frequency of the absorber is slightly detuned from that of the main structure, the explicit forms of the modal parameters of the system and the envelope of the Green's function for the transient response of the main structure are derived according to a perturbation technique. Applying these perturbation solutions, the ratio of the envelope for the main mass with the absorber to that without absorber can be easily constructed and thereby provides an insight to evaluate the effectiveness of the absorber to decrease the vibration of the main mass.

The envelope ratio starts from unity and decreases with increasing time, which implies that the absorber is not effective in decreasing the vibration in the first one or two periods of structural vibration. If the frequency difference between the absorber and the main mass is increased, the envelope ratio has a smaller rate of decay and the absorber becomes less effective. Suitable absorber damping occurs in the range $0 < \xi_d < \sqrt{\gamma}$. Although the envelope ratio has a more rapid exponential decay when ξ_d is near $\sqrt{\gamma}$, a smaller value of ξ_d causes an earlier decay in the curve of the envelope ratio, which leads to a smaller ξ_d having a smaller envelope ratio in the first few periods of structural vibration. However, the curve of envelope ratio for smaller value of ξ_d has an earlier rebound. Therefore, the optimum choice of ξ_d is based on a compromise between an earlier decay and a later rebound.

ACKNOWLEDGEMENTS

The author would like to express his appreciations to Professor G. B. Warburton, the general editor of this journal, for giving suggestions in revising this manuscript. The research work reported in this paper was supported by the National Science Council, Republic of China, under Contract No. NSC 80-0410-E011-02.

REFERENCES

1. J. P. Den Hartog, *Mechanical Vibrations*, 4th edn, McGraw-Hill, New York, 1956.
2. A. G. Thompson, 'Optimum tuning and damping of a dynamic vibration absorber applied to a force excited and damped primary system', *J. sound vib.* **77**, 403–415 (1981).
3. G. B. Warburton, 'Optimum absorber parameters for various combinations of response and excitation parameters', *Earthquake eng. struct. dyn.* **10**, 381–401 (1982).
4. H.-C. Tsai and G.-C. Lin, 'Optimum tuned-mass dampers for minimizing steady-state response of support-excited and damped system', *Earthquake eng. struct. dyn.* **22**, 957–973 (1993).

5. H.-C. Tsai and G.-C. Lin, 'Explicit formulae for optimum absorber parameters for force-excited and viscously damped systems', *J. sound vib.* **176**, 585–596 (1994).
6. H.-C. Tsai, 'Green's function of support-excited structures with tuned-mass dampers derived by a perturbation method', *Earthquake eng. struct. dyn.* **22**, 975–990 (1993).
7. A. S. Veletsos and C. E. Ventura, 'Modal analysis of non-classically damped linear system', *Earthquake eng. struct. dyn.* **14**, 217–243 (1986).
8. J. L. Sackman and J. M. Kelly, 'Seismic analysis of internal equipment and components in structures', *Engineering struct.* **1**, 179–190 (1979).
9. T. Igusa and A. Der Kiureghian, 'Dynamic characterization of two-degree-of-freedom equipment-structure systems', *J. eng. mech. div. ASCE* **111**, 1–19 (1985).
10. Y. Fujino and M. Abé, 'Design formulas for tuned mass dampers based on a perturbation technique', *Earthquake eng. struct. dyn.* **22**, 833–854 (1993).
11. H.-C. Tsai, 'The effect of tuned-mass dampers on the seismic response of base-isolated structures', *Int. j. solids struct.* **32**, 1195–1210 (1995).